Sven Schröder, Wolfgang Frey and Gerhard Maas*

# 2-(1,2,3-Triazol-4-yl)-imidazoline, -oxazoline, -thiazoline and -tetrahydropyrimidine as ligands in copper(II) and nickel(II) complexes

DOI 10.1515/znb-2016-0026
Received February 1, 2016; accepted February 9, 2016

**Abstract:** 2-(1-Benzyl-1*H*-1,2,3-triazol-4-yl)-imidazolines (**L1** and **L2**/**L2′**), -1,3-oxazoline (**L3**), -1,3-thiazoline (**L4**) and -tetrahydropyrimidine (**L5**) were prepared in one step from a 1,2,3-triazole-4-carboxamidinium tetraphenylborate and studied as novel ligands for copper(II) and nickel(II) ions. The solid-state structures of the following complexes were established: $[Cu(\mathbf{L1})_2](OTf)_2$, $[Cu\mathbf{L2L2'}(OTf)_2] \cdot 2H_2O$, $[[Cu(\mathbf{L4})_2(H_2O)_2](OTf)_2 \cdot [Cu(\mathbf{L4})_2(OTf)_2]$, $[Cu(\mathbf{L5})_2(OTf)_2]$, $Cu(\mathbf{L3})_2Cl_2] \cdot THF$, $[Ni(\mathbf{L1})_2Cl_2]$.

**Keywords:** amidinium salt; bidentate ligands; copper complexes; copper(II) triflate; nickel complex; 1,2,3-triazoles.

## 1 Introduction

The ability of aromatic five-membered heterocycles with three or four nitrogen atoms – 1,2,3-triazoles, 1,2,4-triazoles and tetrazoles – to act as ligands in coordination chemistry has been known for a long time. The rather simple synthetic access to these ring systems, enabling also the preparation of a broad range of substituted derivatives, has meanwhile led to a considerable collection of triazole- [1, 2] and tetrazole-containing [1, 3–5] ligands for metal complexation with diverse coordination motifs. As far as 1,2,3-triazoles are concerned, the recent advent of the copper(I)-catalyzed version of the azide–alkyne [3+2] cycloaddition (CuAAC), due to its operative simplicity, mild reaction conditions and regioselectivity [6], has spurred the interest in 1,2,3-triazole containing ligands and their use for diverse functional metal coordination compounds such as spin-crossover complexes, light-emitting materials, sensitizers in dye-sensitized solar cells, radiolabeled pharmaceuticals and building blocks for discrete or polymeric supramolecular architectures (for reviews and selected examples, see Refs. [1, 7–12]). Another interesting development is found in the field of organometallic complexes with triazole-derived ligands, in particular complexes of various transition metals with 1,3,4- or 1,2,4-trisubstituted 1,2,3-triazol-5-ylidene ligands, which have recently been shown to catalyze effectively several important organic transformations as well as photocatalytic water oxidation [13].

Complexes with bidentate N^N chelating ligands incorporating a 1,2,3-triazole moiety have also been found to be catalytically active. Thus, several palladium complexes with (2-pyridyl)-1,2,3-triazole ligands (**1**, Fig. 1) were found to catalyze effectively some modern C,C coupling reactions, namely Suzuki–Miyaura, Sonogashira and Heck reactions [14]. Some triazole-containing compounds are useful rate-enhancing co-ligands for the CuAAC reaction [15]. For example, copper complexes formed from $CuCl_2$ and triazole ligands of the type **2** exhibited good to very good performance in catalyzing this reaction [16]. An octahedral $NiBr_2$ complex with a tetradentate 1,2,3-triazole/acenaphthene quinone diimine ligand was found to be an efficient precatalyst for the MAO induced polymerization of styrene [17].

In a way, the atom connectivity in the first coordination sphere of bidentate ligands **1** is reminiscent of that in bis(1,3-oxazolines) **3**, which in their enantiomerically pure chiral version have contributed to impressive enantioselectivities in several copper-catalyzed asymmetric transformations, as shown in the pioneering studies by the groups of Pfaltz [18], Masamune [19, 20] and Evans [21, 22]. Being interested in novel triazole-derived chelating ligands and their copper complexes, we aimed at conjugates of the ring systems of 1,2,3-triazole and cyclic amidines (i.e. imidazoline and tetrahydropyrimidine), 1,3-oxazoline and 1,3-thiazoline. Results of these studies are reported herein. Notably, heterocyclic conjugates of this type are almost unknown. A synthetic access, different from ours [23], to the triazole-oxazoline scaffold **L3** (see Scheme 1) has been published [23]. Also, several

***Corresponding author: Gerhard Maas,** Institute of Organic Chemistry I, University of Ulm, 89081 Ulm, Germany,
Fax: +49 (0)731 5022803, E-mail: gerhard.maas@uni-ulm.de
**Sven Schröder:** Institute of Organic Chemistry I, University of Ulm, 89081 Ulm, Germany
**Wolfgang Frey:** Institute of Organic Chemistry, University of Stuttgart, Pfaffenwaldring 55, 70569 Stuttgart, Germany

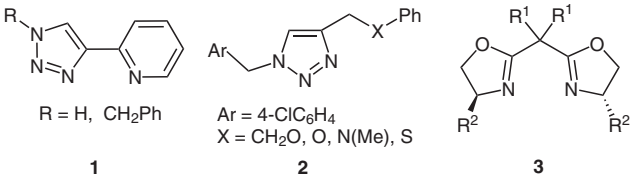


**Fig. 1:** Examples of bidentate ligands for catalytically active complexes.

(1,2,3-triazol-1-yl)-(1,3-oxazol-2-yl and 1,3-thiazol-2-yl) methane derivatives have been synthesized very recently [25]. In both cases, however, no complex formation studies were performed.

# 2 Results and discussion

## 2.1 Syntheses

In a preceding paper, we have reported the preparation of the 1,2,3-triazole-carboxamidinium tetraphenylborate **1** and its one-step conversion into the 2-(1,2,3-triazol-4-yl)imidazoline **L1** [24]. In an analogous manner, we have now combined salt **1** with enantiomerically pure (*R*)-propane-1,2-diamine to provide the chiral triazole/imidazoline hybride ligand **L2** (Scheme 1). The condensation of salt **1** with 2-aminoethanol, 2-aminoethanethiol and propane-1,3-diamine provided the corresponding triazolyl-substituted 1,3-oxazoline **L3**, 1,3-thiazoline **L4** and tetrahydropyrimidine **L5**, all of which were formed in high yield (Scheme 1).

Dynamic prototropic equilibria are present in the cases of cyclic amidine ligands **L1**, **L2** and **L5**, as indicated by broadening of the $^{1}H$ and/or $^{13}C$ NMR signals of the N*CH*$_2$ (and N*CH*) nuclei. Only in the case of **L2**, however, does proton tautomerism lead to structurally different tautomers (**L2** and **L2′**), which are both incorporated in a complex with Cu(OTf)$_2$ (*vide infra*).

## 2.2 Complex formation with copper(II) triflate

Copper(II) trifluoromethanesulfonate (triflate) is sufficiently soluble in several common aprotic-polar organic solvents, so that complexation with organic ligands can take place in a homogeneous medium. Water, which could also act as a ligand, can be excluded *a priori*. Nevertheless, adventitious water in some cases was incorporated into the complex itself or in the crystal lattice during crystallization attempts or exposure to air of the first formed solid complex. Figure 2 shows the structures of the Cu(OTf)$_2$ derived complexes, the solid-state structures of which could be established by single-crystal X-ray structure determination. In all complexes derived from Cu(OTf)$_2$, the organic ligands act as bidentate chelating ones, coordinating to the copper(II) ion at the 1*H*-triazole ring position N-3 and at the imine nitrogen atom of the cyclic amidine or a related ring system. On the other hand, the coordination of the triflate anion, which is known as being a weakly coordinating ion in metal triflates and triflato complexes [26], is subject to variations depending on the particular complex.

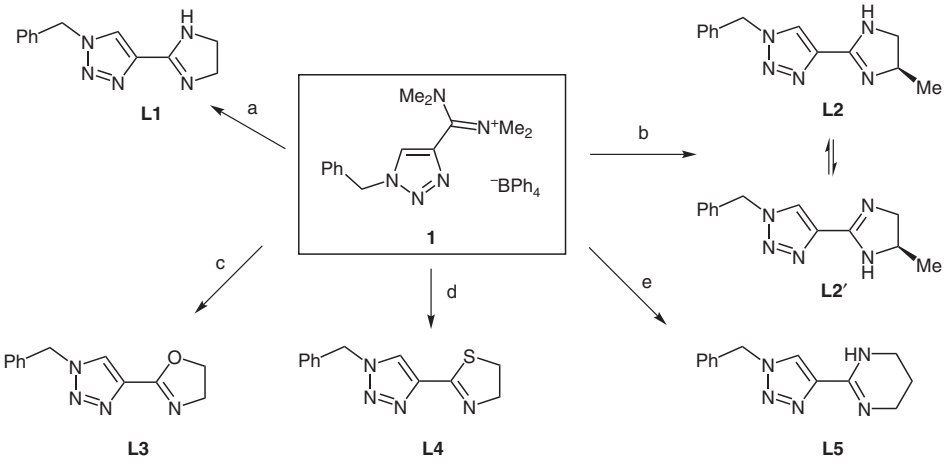


**Scheme 1:** Synthesis of ligands **L1**–**L5**. Conditions and yields: (a) $H_2N(CH_2)_2NH_2$, anhydrous $K_3PO_4$, $CH_3CN$, rfx, 5 h, 92% [24]; (b) (*R*)-propane-1,2-diamine, anhydrous $K_3PO_4$, $CH_3CN$, rfx, 12 h, 92%; (c) $HO(CH_2)_2NH_2$, anhydrous $K_3PO_4$, $CH_3CN$, rfx, 18 h, 88%; (d) $HS(CH_2)_2NH_2$, anhydrous $K_3PO_4$, $CH_3CN$, rfx, 24 h, 88%; (e) $H_2N(CH_2)_3NH_2$, anhydrous $K_3PO_4$, $CH_3CN$, rfx, 18 h, 91%.

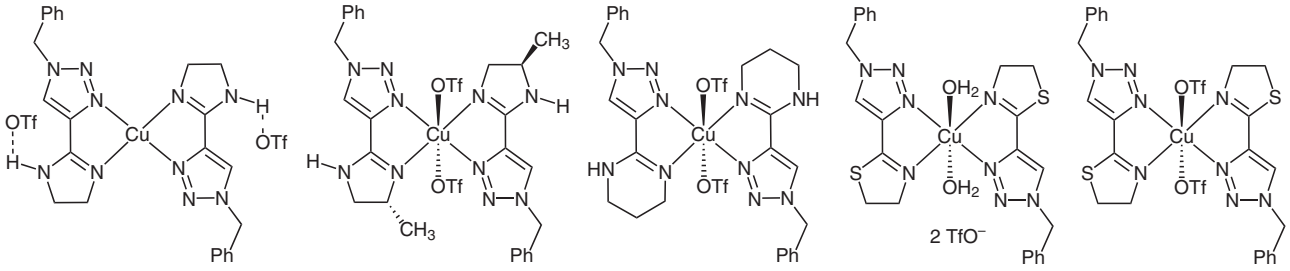


**Fig. 2:** $Cu(OTf)_2$ derived complexes that were structurally characterized in this study (OTf = $O_3SCF_3$).

By concentration of an ethyl acetate solution of $Cu(OTf)_2$ and ligand **L1**, light brown crystals were obtained, the X-ray structure determination of which established the composition $[Cu(\mathbf{L1})_2](OTf)_2$ (Fig. 3). This complex exhibits crystallographic inversion symmetry; four nitrogen atoms (two of each ligand) surround the copper ion in a distorted square-planar geometry (Table 1). The two triflate anions, which are both slightly disordered by rotation

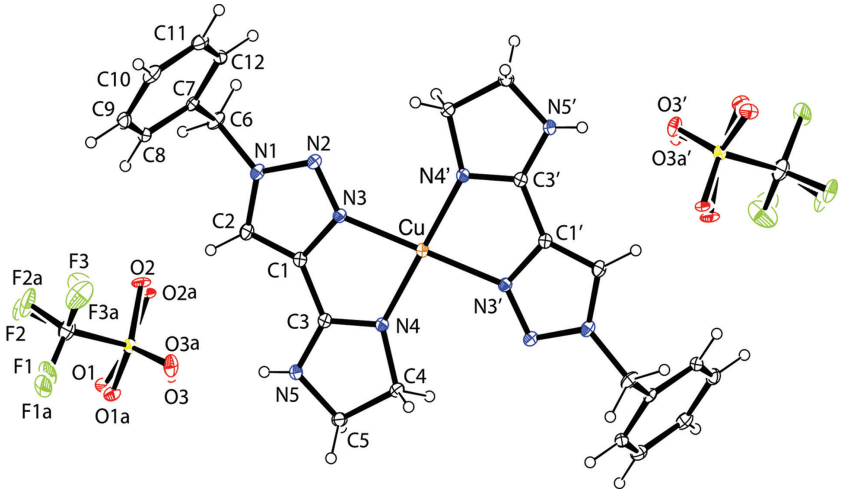


**Fig. 3:** Molecular structure of complex $[Cu(\mathbf{L1})_2](OTf)_2$ in the solid state (ORTEP plot).

**Table 1:** Selected bond lengths (Å) and angles (deg) in $Cu(OTf)_2$ derived complexes.

| $[Cu(L1)_2](OTf)_2$ | $[CuL2L2'(OTf)_2]\times 2H_2O$ | $[Cu(L5)_2](OTf)_2$ | $[Cu(L4)_2(H_2O)_2](OTf)_2$ | $[Cu(L4)_2OTf)_2]$ |
|---|---|---|---|---|
| $Cu-N3_{triaz}$ 2.028(1) | $Cu1-N1_{triaz}$ 2.014(4) | $Cu-N1_{triaz}$ 2.041(2) | $Cu1-N2_{triaz}$ 2.038(2) | $Cu2-N7_{triaz}$ 1.988(3) |
| $Cu-N3'_{triaz}$ 2.028(1) | $Cu1-N6_{triaz}$ 2.015(4) | $Cu-N6_{triaz}$ 2.030(2) | $Cu1-N2'_{triaz}$ 2.038(2) | $Cu2-N7'_{triaz}$ 1.988(3) |
| $Cu-N4_{imid}$ 1.934(1) | $Cu1-N4_{imid}$ 1.951(4) | $Cu-N4_{pyrim}$ 1.977(3) | $Cu1-N1_{thiaz}$ 1.991(2) | $Cu2-N5_{thiaz}$ 2.004(2) |
| $Cu-N4'_{imid}$ 1.934(1) | $Cu1-N9_{imid}$ 1.967(4) | $Cu-N9_{pyrim}$ 1.982(3) | $Cu1-N1'_{thiaz}$ 1.991(2) | $Cu2-N5'_{thiaz}$ 2.004(2) |
| $C3-N4_{imid}$ 1.306(2) | $C3-N4_{imid}$ 1.308(6) | $C16-N9_{pyrim}$ 1.297(4) | $C3-N1_{thiaz}$ 1.275(4) | $C15-N5_{thiaz}$ 1.283(4) |
| | $C17-N9_{imid}$ 1.285(6) | | | |
| N3–Cu–N3′ 180.00(5) | N1–Cu1–N6 177.70(16) | N1–Cu–N6 179.12(10) | N2–Cu1–N2′ 180.00(14) | N7–Cu2–N7′ 180.00(10) |
| N3–Cu–N4 81.89(5) | N1–Cu1–N4 81.27(17) | N1–Cu–N4 81.30(10) | N2–Cu1–N1 81.22(10) | N7–Cu2–N5 81.16(10) |
| N3–Cu–N4′ 98.11(5) | N1–Cu1–N9 99.37(15) | N1–Cu–N9 98.66(10) | N2–Cu1–N1′ 98.78(10) | N7–Cu2–N5′ 98.84(10) |
| N4–Cu–N4′ 180.00(5) | N6–Cu1–N9 81.19(17) | N6–Cu–N9 81.08(10) | N1–Cu1–N1′ 180.00(18) | N5–Cu2–N5′ 180.00(10) |
| C3–N4–Cu 115.5(1) | C3–N4–Cu1 116.3(3) | C3–N4–Cu 115.9(2) | C3–N1–Cu1 115.1(2) | C15–N5–Cu2 114.3(2) |
| C1–N3–Cu 111.6(1) | C2–N1–Cu1 112.7(3) | C2–N1–Cu 110.8(2) | C4–N2–Cu1 111.0(2) | C16–N7–Cu2 113.3(2) |
| | Cu1···O1 2.602(3) | Cu···O1 2.689(2) | Cu1···O1 2.371(3) | Cu2···O4 2.441(2) |
| | Cu1···O4 2.620(3) | Cu···O6 2.535(2) | Cu1···O1′ 2.371(3) | Cu2···O4′ 2.441(2) |
| | O1···Cu1···O4 177.59(4) | O1···Cu···O6 163.12(8) | O1···Cu1···O1′ 180.0(2) | O4···Cu2···O4′ 180.0(2) |

around the C–S bond, are not associated with the metal, but are engaged in an O···H–N hydrogen bond to the imidazoline ring of both organic ligands ($d$(O···N) = 2.83(3)–2.86(3) Å). Additionally, weak interactions of the O···H–C type between a triflate oxygen atom and $CH_{triazole}$ ($d$(O···H) ~2.35 Å) and $m$-$CH_{phenyl}$ (~2.42 Å) may be present.

The blue crystals obtained from Cu(OTf)$_2$ and ligand (*R*)-**L2**/(*R*)-**L2′** by crystallization from ethyl acetate-diethyl ether showed the expected 1:2 metal-to-ligand ratio; surprisingly, however, an X-ray structure determination revealed the composition [Cu**L2L2′**(OTf)$_2$] · 2$H_2O$, i.e. a complex molecule containing both imidazoline tautomers, (*R*)-**L2** and (*R*)-**L2′** (Fig. 4, top). The copper(II) ion is surrounded by four nitrogen atoms in a distorted square-planar geometry which is extended into a tetragonally distorted octahedral arrangement by two weakly coordinated triflate anions (Cu1···O1 2.602(3), Cu1···O4 2.620(3) Å)). Notably, the triflate anions do not maintain O···H–N

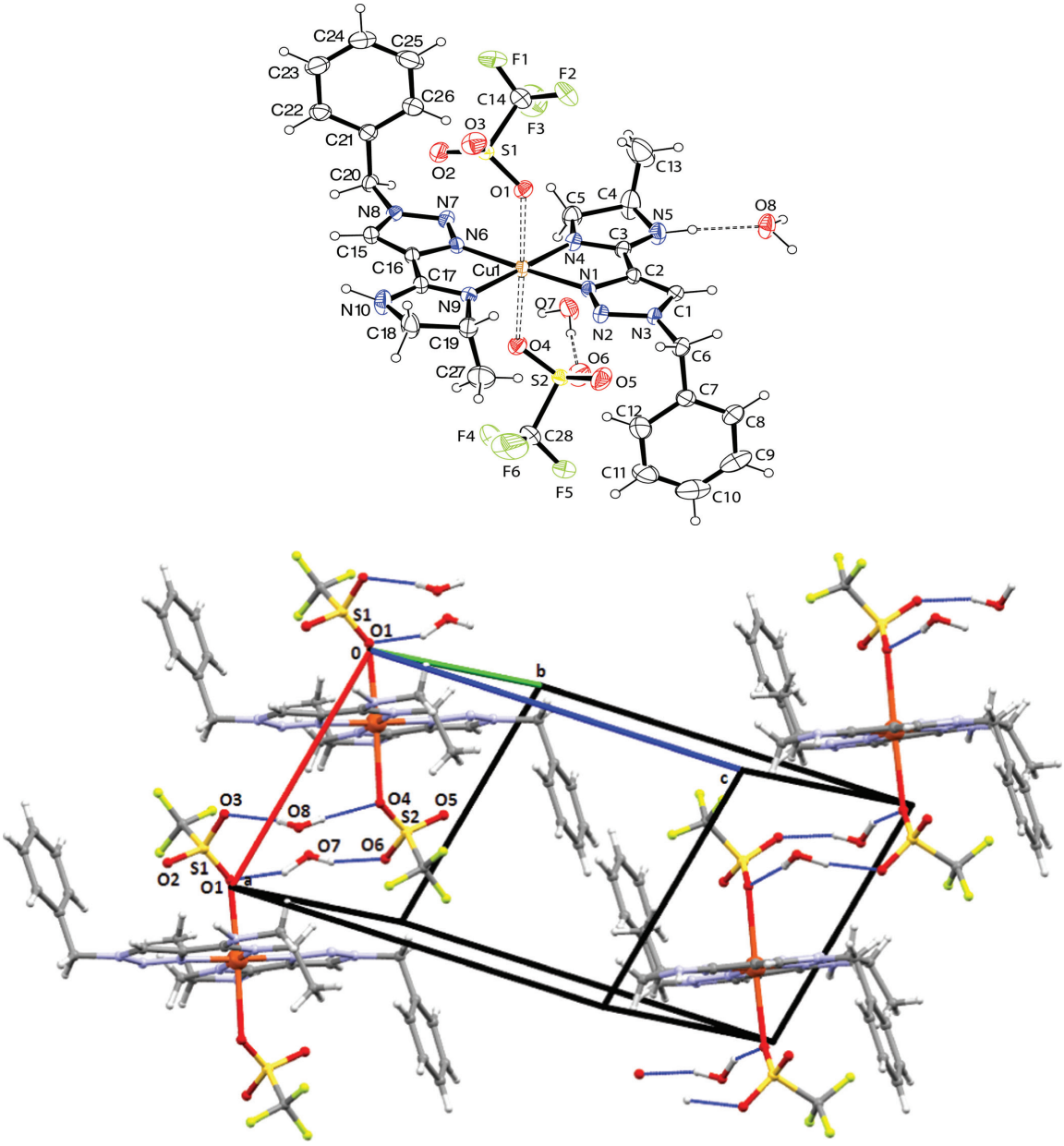


**Fig. 4:** Top: molecular structure of complex [Cu**L2L2′**(OTf)$_2$] · 2 $H_2O$ in the solid state (ORTEP plot). Bottom: water molecules involved in O–H···O hydrogen bonds; for clarity, $N_{imidazoline}$–H···O bonds involving the water molecules are not shown (MERCURY plot). Geometrical data ($d$(D···A), angle D–H···A; D = donor, A = acceptor) for N5–H···O8: 2.811(7) Å, 157°; for N10–H···O7: 2.768(8) Å, 157°; for O7–$H^A$···O1: 2.841(7) Å, 155°; for O7–$H^B$···O6 2.756(7) Å, 163°; for O8–$H^A$···O3: 2.834(8) Å, 150°; for O8–$H^B$···O4: 2.872(7) Å, 169°.

hydrogen bonds with the imidazoline rings of neighboring ligands. Rather, two water molecules, which are present in the asymmetric unit of the crystal, connect two triflate ions via O···H–O bonds (Fig. 4, bottom) and each of them is associated with an imidazoline ring via an O···H–N hydrogen bond.

Blue crystals of a complex formed from $Cu(OTf)_2$ and triazolyl-tetrahydropyrimidine **L5** were obtained by slow diffusion of diethyl ether into an *n*-butanol solution of the components; crystallization attempts from other solvents or solvent mixtures were unsuccessful. According to an X-ray analysis, the complex $[Cu(\mathbf{L5})_2(OTf)_2]$ had been formed (Fig. 5, top). Similar to the complex with the triazolyl-imidazoline ligand **L2**/**L2′**, a distorted octahedral coordination geometry with the two triflate ions occupying the apical positions is observed (Table 1). The two copper–oxygen distances are rather long again, and additionally, they differ more from each other and the O···Cu···O angle is farther away from linearity. Besides using one oxygen atom for coordination to the copper atom, each triflate group is engaged with a second oxygen atom in an O···H–N hydrogen bond to the amidine NH group of another complex molecule (Fig. 5, bottom).

When a solution of $Cu(OTf)_2$ and ligand **L4** in ethyl acetate was slowly concentrated by solvent evaporation with exposure to air, light blue crystals were formed, which analyzed for the composition $Cu(\mathbf{L4})_2(OTf)_2(H_2O)$ but according to an X-ray analysis were in fact 1:1 cocrystals of two different complexes, namely a diaqua and a bis(triflato) copper(II) complex, $[Cu(\mathbf{L4})_2(H_2O)_2](OTf)_2 \cdot [Cu(\mathbf{L4})_2(OTf)_2]$ (Fig. 6). Both complex entities are centrosymmetrical with the copper ion on a crystallographic

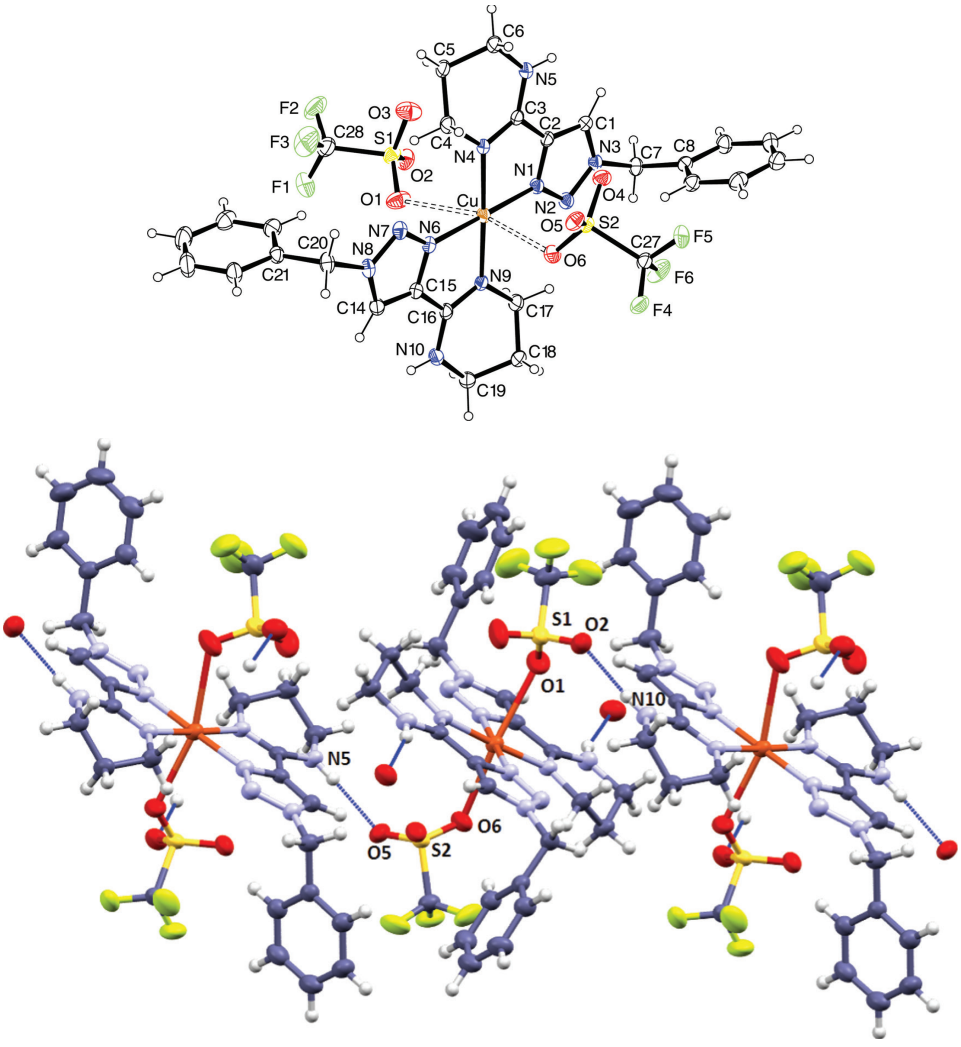


**Fig. 5:** Top: molecular structure of complex $[Cu(\mathbf{L5})_2(OTf)_2]$ in the solid state (ORTEP plot). Bottom: N–H···O hydrogen bonding in the crystal structure (MERCURY plot). Geometrical data (*d*(N–H), *d*(H···O), *d*(N···O), angle N–H···O) for N5–H5···O5: 0.83, 2.08, 2.895(3), 164(3)°; for N10–H10···O2: 0.83, 2.03, 2.821(4), 159(4)°.

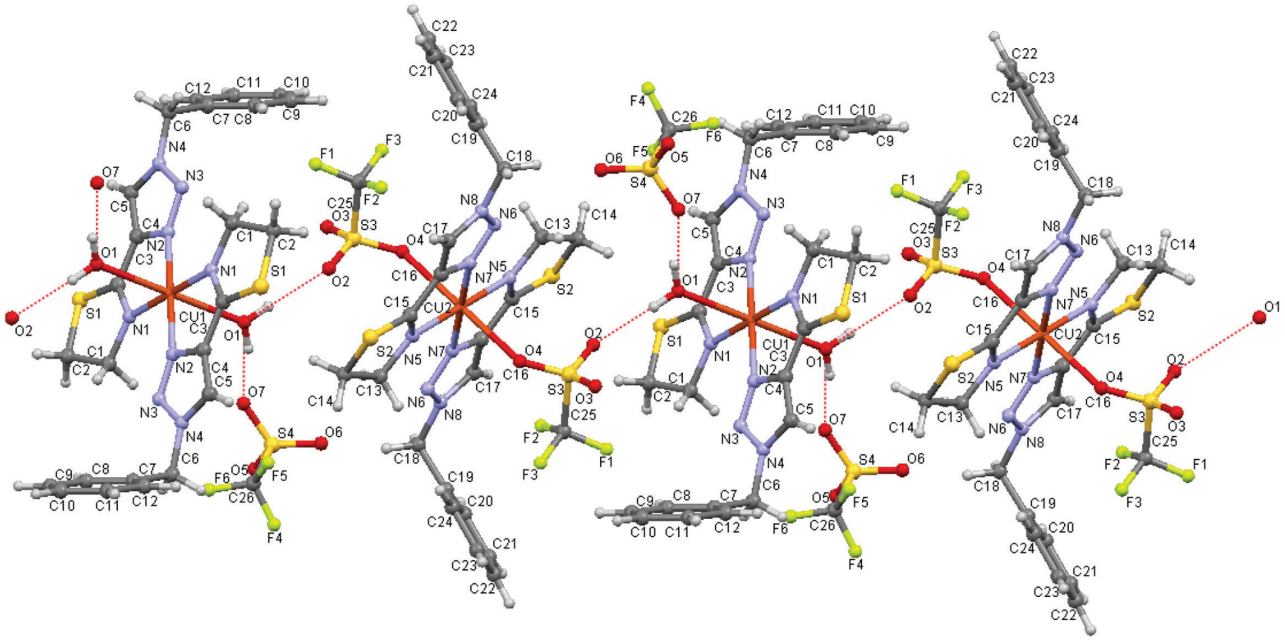

**Fig. 6:** Molecular structure and packing of complex $[Cu(\mathbf{L4})_2(H_2O)_2](OTf)_2$/$[Cu(\mathbf{L4})_2(OTf)_2]$ in the solid state (ORTEP plot). Geometrical data (*d*(D–H), *d*(H···A), *d*(D···A), angle D–H···A; D = donor, A = acceptor) for O1–$H^A$···O2: 0.82(4), 2.06(4), 2.826(4), 155(4)°; for O1–$H^B$···O7: 0.86(5), 1.90(5), 2.742(4), 168(4)°.

inversion center. The coordination geometries can be described as distorted octahedral with the oxygen ligands in the apical positions. The Cu···O distances amount to 2.371(3) Å in the diaqua complex and 2.441(2) Å in the bis(triflato) complex. Although the triflate coordination may be rather weak, the contact distance is the shortest one among the triflato complexes presented here. In notable contrast to all other complexes, the $Cu–N_{triazole}$ and $Cu–N_{thiazole}$ distances are almost equal in $[Cu(\mathbf{L4})_2OTf)_2]$, and moreover, the $Cu–N_{triazole}$ bonds are even slightly longer. The two complex entities in the crystals are connected through hydrogen bonds between the water ligands of the diaqua complex and a triflate oxygen atom of the bis(triflato) complex. The two triflate anions, which compensate the positive charge of the diaqua complex, are each involved in one hydrogen bond with a water ligand but remain uncoordinated otherwise.

In the IR spectra of the complexes, absorption bands in the 1540–1650 $cm^{-1}$ region, attributable to vibrations in the triazole and the second heterocyclic ring, are significantly displaced compared to the free ligands. In detail, the C=N stretching vibrations of the imidazoline, oxazoline, thiazoline and tetrahydropyrimidine rings appear between 1625 and 1640 $cm^{-1}$ in the free ligands and are shifted to higher wavenumbers in the complexes containing the cyclic amidine ligands and to lower ones in the oxazoline and thiazoline complexes. Absorption bands of the *N*-benzyl-1,2,3-triazole part of the ligands are found in the range 1531–1573 $cm^{-1}$ for the free ligands, but at higher wavenumbers (by 12–40 $cm^{-1}$) in the complexes, except for $Cu(\mathbf{L3})_2Cl_2$, where the triazole part remains uncoordinated (*vide infra*). Of particular interest is the region between 1300 and 1000 $cm^{-1}$, where strong absorptions associated with stretching modes of the $CF_3SO_3$ group dominate. In the past, the assignment of the vibration modes of the triflate group has found much attention, mainly in order to distinguish between a free and a coordinated triflate ion. When a triflate ion becomes mono- or di-coordinated – either to a metal atom or by a strong hydrogen bond – the $C_{3v}$ symmetry of the free triflate ion is reduced to $C_s$, resulting in a splitting of the E type vibrations. Thus, the asymmetric stretching vibration of the $SO_3$ group, which appears around 1270 $cm^{-1}$ for the uncoordinated triflate [27], is expected to be split. This splitting was observed indeed in a number of triflate-containing copper complexes, the solid-state structures of which have been determined. Following the established assignment of the relevant vibration modes of the triflate ion (for examples, see lit. [27–32]), the assignments shown in Table 2 were made for the $Cu(OTf)_2$ complexes under study. It can be seen, that splitting of the $\nu_{as}(SO_3)$ vibration is observed in all cases, including complex $[Cu(\mathbf{L1})_2](OTf)_2$, where the triflate ions are involved in N–H···O hydrogen bonding according to the crystal structure analysis, but not in metal coordination. As we have indicated in Table 2, some of the

**Table 2:** IR vibrations associated with the $CF_3SO_3$ ion in the copper(II) triflate complexes under study (wavenumbers, $cm^{-1}$).[a,b]

| Vibration | $Cu(L1)_2](OTf)_2$ | $[CuL2L2'(OTf)_2]$ | $[Cu(L5)_2](OTf)_2$ | $[Cu(L4)_2(H_2O)_2](OTf)_2$ $[Cu(L4)_2OTf)_2]$ |
|---|---|---|---|---|
| $\nu_{as}(SO_3)$ | 1296/1253 | 1285/1243 | 1284/1256 | 1286/1246 |
| $\nu_s(CF_3)$ | 1228* | ~1225–1230 sh | 1225* | 1224* |
| $\nu_{as}(CF_3)$ | 1148 | 1159 | 1167 | 1158 |
| $\nu_s(SO_3)$ | 1029 | 1028 | 1032 | 1028 |
| $\delta_s(CF_3) + \nu_s(CS)$[c] | 757 | | 759 | |
| $\delta_s(SO_3)$ | 629 | 636 | 637 | 639 |
| $\delta_{as}(CF_3)$ | 575 | 574 | 576 | 576* |
| $\delta_{as}(SO_3)$ | 520 | 518 | 518 | 518 |

[a]Spectra were recorded from KBr pellets; [b]absorptions marked with an asterisk appear at the same wavenumber as an absorption of the free ligand; [c]the $\delta_s(CF_3)$ absorption, which should appear around 752 $cm^{-1}$ [27] and has been described as "weak" or "medium" in the literature, could not be identified with certainty. Only in two cases, weak absorptions were observed at approximately this wavenumber.

absorption bands arising from the triflate ions appear at more or less the same wavenumber as absorptions also observed for the free ligand, but due to the high intensity of the triflate absorption bands, the assignment is unequivocal.

Electronic spectra of some of the $Cu(OTf)_2$ complexes were recorded. For solubility reasons, acetonitrile had to be used as the solvent; since no visible color change was noted between the complexes in the solid state and in solution, we can assume that acetonitrile molecules did not replace the triflate ions as ligands. The spectra display two absorption maxima above 350 nm, which are not present in the spectra of the free ligands: one around 370–380 nm, belonging to a broadened absorption that extends into the visible region and in some cases includes a shoulder at the longer wavelength side, and the other one as a very broad, low-intensity absorption in the visible region with maxima in the range of 608–664 nm (Table 3). The latter absorption band is unsymmetrical, with a long tailing up to about 950 nm. Absorptions in this range are commonly assigned to ligand-field transitions within tetragonally distorted octahedral Cu(II) complexes. [28, 33]. The absorption at higher energy is likely to arise from a $\pi$(ligand)-*d*(Cu(II)) charge transfer transition [28].

**Table 3:** Electronic absorption bands of some complexes in acetonitrile solution.

| Complex | $\lambda_{max}$ ($\varepsilon$ in L $mol^{-1}$ $cm^{-1}$) |
|---|---|
| $[Cu(\mathbf{L1})_2](OTf)_2$ | 368 (239), ~415 (sh, 171), 643 (72) |
| $[Cu\mathbf{L2L2'}(OTf)_2]$ | 371 (259), 656 (64) |
| $[[Cu(\mathbf{L4})_2(H_2O)_2](OTf)_2 \cdot$ $[Cu(\mathbf{L4})_2OTf)_2]$ | 364 (245), 664 (70) |
| $[Cu(\mathbf{L5})_2](OTf)_2$ | 370 (sh, 168), 608 (87) |
| $[Cu(\mathbf{L3})_2]Cl_2$ | 375 (264), ~420 (sh, 225), 748 (118) |

## 2.3 Complexes with $CuCl_2$ and $NiCl_2$

Similar to $Cu(OTf)_2$, $CuCl_2$ is also soluble in a variety of aprotic-polar organic solvents and in the lower aliphatic alcohols. The complexation of solvatochromic $CuCl_2$ by ligand **L1** in several solvents was indicated by a characteristic color change to dark green, but the very thin needle-shaped crystals or amorphous solids obtained were not suited for single-crystal X-ray structure determination.

With the triazole/oxazoline ligand **L3**, on the other hand, copper(II) chloride in tetrahydrofuran formed crystals of the dark blue complex $[Cu(\mathbf{L3})_2Cl_2] \cdot$ THF. In the crystal structure, copper resides on an inversion center and has a square-planar coordination with the symmetry-related ligands in *trans* position (Figs. 7 and 8). The organic ligands coordinate solely at the imine nitrogen atom of the oxazoline ring, but not at the less nucleophilic N1 position of the triazole ring. The structure of the complex is analogous to that of Cu(1-ethyltetrazole-$N^4)_2Br_2$] [34] and also to the complex comprising $CuCl_2$ and ligand **2** (Fig. 1, X = $CH_2O$), $[Cu(\mathbf{2})Cl_2]$, where geometrical constraints obviously do not allow the oxygen atom in the side chain to coordinate to the metal atom [16]. On the other hand, ligand **3** (Fig. 1, $R^1$ = Me, $R^2$ = *tert*-Bu) and $CuCl_2$ form a 1:1 chelate complex with a distorted tetrahedral geometry around the copper atom [35]. Notably, the long-wavelength absorption of our $CuCl_2$/bis(oxazoline) complex appears at $\lambda$ = 748 nm, i.e. with a large batochromic shift compared to the complexes derived from $Cu(OTf)_2$ (Table 2).

The formation of nickel complexes was thwarted by the insufficient solubility of simple nickel salts in common organic solvents. However, crystals of the light green complex $[Ni(\mathbf{L1})_2Cl_2]$ could be obtained in modest yield from nickel(II) chloride and **L1** in *n*-propanol. The

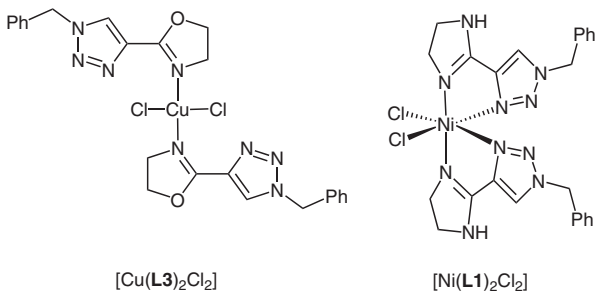


**Fig. 7:** Structural formulae of complexes derived from $CuCl_2$ and $NiCl_2$.

X-ray structure determination revealed a distorted octahedral coordination geometry with the planes of the two ligands **L1** being perpendicular to each other (Figs. 7 and 9). The complex has crystallographic $C_2$ symmetry; the twofold rotation axis bisects the Cl–Ni–Cl′ angle. As in most of the copper complexes, the Ni–N(imine) distance is distinctly shorter than the Ni–N(triazole) distance (2.046 vs. 2.172 Å). The crystal packing is stabilized by N–H···Cl hydrogen bonds which connect each chlorine atom of a complex molecule with the imidazoline rings of another molecule.

## 3 Conclusion

In this study, we have used amidinium chemistry for the synthesis of 2-(1,2,3-triazol-4-yl)-imidazoline, -oxazoline,

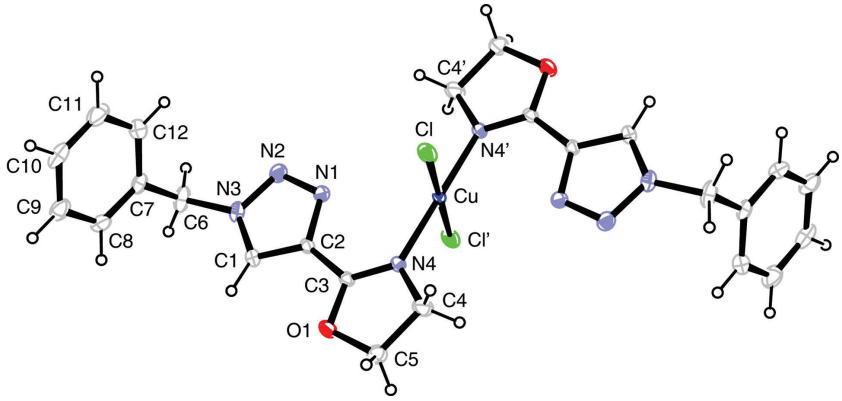


**Fig. 8:** Molecular structure of complex $[Cu(\mathbf{L3})_2Cl_2] \cdot THF$ in the solid state (Ortep plot). The positionally disordered tetrahydrofuran molecule is not shown. Selected bond lengths and angles: Cu–N4 = Cu–N4′ 1.957(2), Cu–Cl = Cu–Cl′ 2.2957(6), C3–N4 1.277(3) Å; N4–Cu–N4′ 180.00(4), Cl–Cu–Cl′ 180.00(3), N4–Cu–Cl 89.40(5), N4′–Cu–Cl 90.60(5), C3–N4–Cu 128.51(15)°.

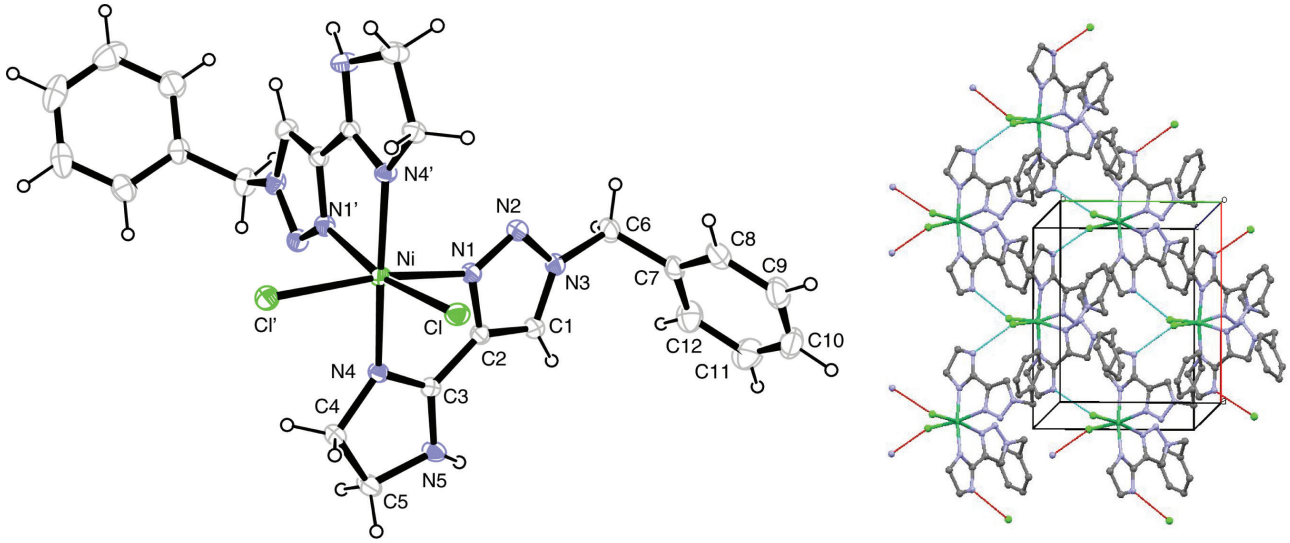


**Fig. 9:** Left: molecular structure of complex $[Ni(\mathbf{L1})_2Cl_2]$ in the solid state (Ortep plot). Selected bond lengths and angles: Ni–N1 = Ni–N1′ 2.1723(14), Ni–N4 = Ni–N4′ 2.0460(13), Ni–Cl = Ni–Cl′ 2.4186(5), C3–N4 1.294(2) Å; N1–Ni–N1′ 88.03(7), N1–Ni–Cl 88.51(4), N1–Ni–Cl′ 168.82(4), Cl–Ni–Cl′ 96.78(2), N1–Ni–N4 95.71(5), N4–Ni–N4′ 171.63(8), Ni–N1–C2 110.92(10), Ni–N4–C3 116.57(11)°. Right: Details of the crystal structure, featuring N–H···Cl hydrogen bonds (Mercury plot). Data for N5–H5N···Cl (*x*–0.5, *y*–0.5, –*z*+1.5): *d*(N–H) 0.88(3) Å, *d*(H···Cl) 2.33(3) Å, *d*(N···Cl) 3.195(2) Å, (N–H···Cl) 167(2)°.

-thiazoline and -tetrahydropyrimidine hybrids. These compounds represent novel bi-heterocyclic ligands for metal complexation, as shown here for Cu(II) and Ni(II) complexes. With $\sigma$ donation by a triazole nitrogen atom and the imine-type nitrogen atom of the other heterocyclic ring, these ligands in principle can act as bidentate chelating ones. This was observed indeed for all structurally characterized copper(II) triflate complexes as well as for the octahedral complex [Ni(**L1**)$_2$Cl$_2$]. Only in the CuCl$_2$–bis(oxazoline) complex *trans*-[Cu(**L3**)Cl$_2$], the organic ligand is monodentate and coordinates at the imine-type nitrogen atom only.

The triflate ion is known as a weakly coordinating anion. This is confirmed in the solid-state structures of the Cu(OTf)$_2$ derived complexes studied here. If hydrogen bond donors (OH of water molecules and NH of amidine ligands) are present, they compete or cooperate with the O···Cu coordination. Consequently, we observed the complete absence of triflate-to-metal coordination in the distorted square-planar complex [Cu(**L1**)$_2$](OTf)$_2$. In the other complexes a distorted square-pyramidal coordination around copper with two triflate ions in the apical positions and rather long Cu···O contacts (2.441–2.689 Å), i.e. values much above the sum of the covalence radii (2.20 Å), was found.

While this study has had a focus on structural aspects of copper(II) and nickel(II) complexes with novel 1,2,3-triazole containing biheterocyclic ligands, for which catalytic applications can be foreseen, it should be kept in mind that 1,2,3-triazole moieties can also be incorporated in potentially bioactive compounds [36, 37]. Insofar, the triazole-imidazoline, -oxazoline and -thiazoline scaffolds presented here could also serve as model compounds for the study of biologically relevant metal ion (Cu(II), Zn(II))/ligand interactions. Along these lines, triazolyl-oxazoline **L3**, assuming that it would act as a bidentate chelating ligand for Zn(II), has already been tested as an inhibitor of several metalloproteinases, but showed no such activity [23].

# 4 Experimental section

## 4.1 General information

$^1$H and $^{13}$C NMR spectra were recorded on a Bruker DRX 400 spectrometer ($^1$H: 400.13 MHz; $^{13}$C: 100.61 MHz); $\delta$ values are reported in ppm and coupling constants in Hertz (Hz). The signal of the solvent was used as an internal standard: $\delta$(C*H*Cl$_3$) = 7.26 ppm, $\delta$(*C*DCl$_3$) = 77.0 ppm; CD$_3$OD: 3.31 and 49.0 ppm; [D$_6$]DMSO: 2.50 and 39.5 ppm; CD$_3$CN: 1.94 and 1.30 ppm. – IR spectra: Bruker Vector 22; wavenumbers (cm$^{-1}$) and intensities (vs = very strong, s = strong, m = medium, w = weak, br = broad) are given, spectra were recorded from KBr pellets. – Mass spectra: MALDI-TOF spectra were recorded with a Bruker Daltonics REFLEX III instrument, *trans*-2-(3-(4-*tert*-butylphenyl)-2-methyl-2-propenylidene)malononitrile (DCTB) was used as matrix. Elemental analyses: elementar vario MICRO cube and elementar Vario EL; values are given in percent. Melting points were determined on a Büchi Melting Point B-540 apparatus. Solvents were distilled, dried by standard methods and stored under argon. Column chromatography was performed on silica gel 60 (Macherey–Nagel, 0.063–0.2 mm) or basic activated alumina 90 (Merck).

## 4.2 Syntheses of ligands L1–L5

1-Benzyl-*N*,*N*,*N*′,*N*′-tetramethyl-1,2,3-triazole-4-carboxamidinium tetraphenylborate (**1**) and 1-benzyl-4-(4,5-dihydro-1*H*-imidazol-2-yl)-1*H*-1,2,3-triazole (**L1**) were prepared according to the published procedures [24].

### 4.2.1 (*R*)-1-Benzyl-4-(4-methyl-4,5-dihydro-1*H*-imidazol-2-yl)-1*H*-1,2,3-triazole (L2) and (R)-1-benzyl-4-(5-methyl-4,5-dihydro-1*H*-imidazol-2-yl)-1*H*-1,2,3-triazole (L2′)

To a solution of amidinium salt **1** (288 mg, 0.50 mmol) and (*R*)-1,2-diaminopropane dihydrochloride (88 mg, 0.60 mmol) in dry acetonitrile was added anhydrous K$_3$PO$_4$ (106 mg, 0.50 mmol) and the mixture was heated at reflux for 12 h. After cooling the solvent was evaporated, and a solution of the residue in ethyl acetate-ethanol (9:1 *v*/*v*) was filtered over a column filled with alumina (10 g). The product was isolated as a colorless solid (110 mg, 0.46 mmol; yield: 92%). M.p. 167.5–169°C. – IR (KBr): $\tilde{\nu}$ = 3244 m, 3105 m, 2957 w, 2919 w, 1626 s, 1561 s, 1452 m, 1285 m, 1232 m, 1050 m, 711 m cm$^{-1}$. – $^1$H NMR (CDCl$_3$): $\delta$ = 1.28 (d, $^3J$ = 6.4 Hz, 3 H, CH$_3$), 3.34 (dd, $J$ = 11.4, 7.8 Hz, 1 H, NCH$^A$), 3.88 (dd, $J$ = 11.4, 9.8 Hz, 1 H, NCH$^B$), 4.09–4.18 (centered m, 1 H, NC*H*CH$_3$), 5.03 (very broad, 1 H, NH), 5.54 (s, 2 H, PhCH$_2$), 7.26–7.28 (m, 2 H, H$_{Ph}$), 7.35–7.37 (m, 3 H, H$_{Ph}$), 8.08 (s, 1 H, 5-H$_{triaz}$) ppm. – $^{13}$C NMR ([D$_4$]methanol): $\delta$ = 21.7 (CH$_3$), 54.6 (Ph*C*H$_2$), 56.8 (coalescing, NCH$_2$/NCH), 124.3 (C-5$_{triaz}$); 128.5, 129.2, 129.4, 133.8 (alle C$_{Ph}$); 139.7 (C-4$_{triaz}$), 156.4 (NC=N)

ppm. – Anal. for $C_{13}H_{15}N_5$ (241.13): calcd. C 64.71, H 6.27, N 29.02; found C 64.93, H 6.26, N 28.89.

#### 4.2.2 2-(1-Benzyl-1*H*-1,2,3-triazol-4-yl)-4,5-dihydrooxazole (L3)

To a suspension of amidinium salt **1** (200 mg, 0.35 mmol) and anhydrous $K_3PO_4$ (210 mg, 1.000 mmol) in dry acetonitrile (12 mL) was added freshly distilled 2-aminoethanol (25 µL, 0.40 mmol) and the mixture was kept with stirring at reflux temperature for 18 h. After cooling, the solvent was evaporated *in vacuo*. The residue was dissolved in ethyl acetate–ethanol (87:13 *v*/*v*), alumina (1 g) was added, the solvent mixture was evaporated and the residue was placed on top of a column packed with alumina (40 g). Chromatography with ethyl acetate–ethanol (87:13 *v*/*v*) furnished **L3** as a colorless crystalline solid ($R_f$ = 0.41; yield: 70 mg, 88%). M.p. 174.0–175.6°C. – IR (KBr): $\tilde{\nu}$ = 3134 w, 3036 w, 1671 s, 1552 m, 1496 m, 1460 m, 1397 m, 1367 m, 1290 m, 1246 m, 1213 m, 1195 m, 1140 m, 1102 m, 1053 s, 1004 m, 970 m, 935 m, 890 m, 720 s cm$^{-1}$. – $^1$H NMR ($CDCl_3$): $\delta$ = 4.03 (t, $^3J$ = 9.4 Hz, 2 H, $NCH_2$), 4.44 (t, $^3J$ = 9.5 Hz, 2 H, $OCH_2$), 5.57 (s, 2 H, $PhCH_2$), 7.27–7.30 (m, 2 H, $H_{Ph}$), 7.37–7.40 (m, 3 H, $H_{Ph}$), 7.89 (s, 1 H, 5-$H_{triaz}$) ppm. – $^{13}$C NMR ([$D_4$]methanol): $\delta$ = 54.8, 54.9 ($NCH_2$ and Ph*C*$H_2$); 69.0 ($OCH_2$); 127.2 (C-5$_{triaz}$); 129.0, 129.6, 130.0 (all $C_{Ph}$); 136.1 and 137.8 (C-4$_{triaz}$, $C_{Ph}$), 159.9 (C-2, oxazoline) ppm. – Anal. for $C_{12}H_{12}N_4O$ (228.25): calcd. C 63.15, H 5.30, N 24.55; found C 63.15, H 5.35, N 24.41.

#### 4.2.3 2-(1-Benzyl-1*H*-1,2,3-triazol-4-yl)-4,5-dihydrothiazole (L4)

The preparation of **L4** followed the procedure described above for **L3**, using salt **1** (90 mg, 0.16 mmol), anhydrous $K_3PO_4$ (105 mg, 0.50 mmol) and 2-aminoethanethiol (16 mg, 0.21 mmol) in dry acetonitrile (12 mL). Reaction conditions: 24 h at reflux temperature. Column chromatography with ethyl acetate-ethanol (8:2) as eluent furnished 34 mg (88% yield) of **L4** as a light yellow solid ($R_f$ = 0.53), M.p. 141–143°C. – IR (KBr): $\tilde{\nu}$ = 3138 m, 3001 w, 1627 s, 1531 m, 1496 m, 1455 m, 1428 m, 1301 m, 1229 m, 1168 m, 1039 m, 1001 s, 913 s, 823 m, 771 s, 666 m cm$^{-1}$. – $^1$H NMR ($CDCl_3$): $\delta$ = 3.39 (t, $^3J$ = 8.5 Hz, 2 H, $SCH_2$), 4.38 (t, $^3J$ = 8.5 Hz, 2 H, $NCH_2$), 5.56 (s, 2 H, $PhCH_2$), 7.28–7.30 (m, 2 H, $H_{Ph}$), 7.36–7.40 (m, 3 H, $H_{Ph}$), 7.87 (s, 1 H, 5-$H_{triaz}$) ppm. – $^{13}$C NMR ($CDCl_3$): $\delta$ = 31.9 ($SCH_2$), 53.4 (Ph*C*$H_2$), 63.6 ($NCH_2$), 121.7 (C-5$_{triaz}$); 127.3, 128.0, 128.2, 132.8 (all $C_{Ph}$); 142.0 (C-4$_{triaz}$), 159.6 (C-2$_{thiaz}$) ppm. – Anal. for $C_{12}H_{12}N_4S$ (244.32): calcd. C 58.99, H 4.95, N 22.93; found C 58.84, H 4.99, N 3.08.

#### 4.2.4 2-(1-Benzyl-1*H*-1,2,3-triazol-4-yl)-1,4,5,6-tetrahydropyrimidine (L5)

The preparation of **L5** followed the procedure described above for **L3**, using salt **1** (300 mg, 0.52 mmol), anhydrous $K_3PO_4$ (212 mg, 1.00 mmol) and 1,3-diaminopropane (50 µL, 0.59 mmol) in dry acetonitrile (20 mL). Reaction conditions: 18 h at reflux temperature. Column chromatography with ethyl acetate–ethanol (8:2) as eluent afforded 113 mg (91% yield) of **L5** as a colorless solid ($R_f$ = 0.32), M.p. 157–159°C. – IR (KBr): $\tilde{\nu}$ = 3223 br m, 3150 m, 2936 m, 1630/1626 vs, 1573 vs, 1498 m, 1456 m, 1312 m, 1254 m, 1228 m, 1186 m, 1070 m, 1048 m, 998 m, 712 s, 696 m cm$^{-1}$. – $^1$H NMR ($CDCl_3$): $\delta$ = 1.85 (quin, $^3J$ = 5.7 Hz, 2 H, $CH_2CH_2CH_2$), 3.45 (t, $^3J$ = 5.7 Hz, 4 H, 2 $NCH_2$), 5.49 (s, 2 H, $PhCH_2$), 7.25–7.27 (m, 2 H, $H_{Ph}$), 7.33–7.45 (m, 3 H, $H_{Ph}$), 7.86 (s, 1 H, 5-$H_{triaz}$) ppm. – $^{13}$C NMR ($CDCl_3$): $\delta$ = 21.0 ($CH_2CH_2CH_2$), 41.7 (broadened, $NHCH_2$ and $=NCH_2$), 54.6 ($PhCH_2$), 122.3 (C-5$_{triaz}$); 128.5, 129.0, 129.3, 134.0 (all $C_{Ph}$); 145.3 (C-4$_{triaz}$), 147.8 (NC=N) ppm. – Anal. for $C_{13}H_{15}N_5$ (241.29): calcd. C 64.71, H 6.27, N 29.02; found C 64.48, H 6.18, N 28.64.

### 4.3 Syntheses of complexes

#### 4.3.1 Bis(1-benzyl-4-(4,5-dihydro-1*H*-imidazol-2-yl)-1,2,3-triazole)copper(II) bis(trifluoromethanesulfonate), $[Cu(L1)_2](OTf)_2$

To a solution of ligand **L1** (50 mg, 0.2 mmol) in ethyl acetate (3 mL) was added a saturated solution of copper(II) trifluoromethanesulfonate ($Cu(OTf)_2$) in ethyl acetate (2 mL). A blue-green precipitate appeared within 10 min, which was transformed into green-brown hexagonal crystals during slow evaporation of the solvent on standing with air contact. The crystals were collected by filtration with suction, washed with a small volume of ethyl acetate to remove co-precipitated $Cu(OTf)_2$. Yield: 85 mg (95%); M.p. 272–274°C. – IR (KBr): $\tilde{\nu}$ = 3262 m br (NH), 3147 w, 3103 w, 1645 m, 1597 s, 1296 vs, 1253 vs, 1228 s, 1148 s, 1076 m, 1059 m, 1029 vs, 757 w, 729 s, 629 s, 575 m, 520 m cm$^{-1}$. – MS ((+)-MALDI-TOF): *m*/*z* (%) = 666.24 (100) $[M–CF_3SO_3]^+$, 516.26 (15) $[M–2CF_3SO_3–H]^+$, 228.16 (74) [**L1**+H]$^+$. – Anal. for $C_{26}H_{26}CuF_6N_{10}O_6S_2$ (816.21): calcd. C 38.26, H 3.21, N 17.16; found C 38.25, H 3.49, N 16.92.

#### 4.3.2 [CuL2L2′(OTf)$_2$] · 2 H$_2$O

Ligand **L2**/**L2′** (15.2 mg, 63 µmol) was dissolved in ethyl acetate (5 mL) and a solution of Cu(OTf)$_2$ (11.4 mg, 31.5 µmol) in ethyl acetate (3 mL) was added. The blue precipitate was isolated by filtration with suction and dried at air; yield: 26 mg (98%). Crystals suitable for X-ray diffraction analysis were obtained when a solution of the precipitate in the necessary amount of ethyl acetate was concentrated by slow evaporation. M.p. 255.5–256.5°C. – IR (KBr): IR (KBr): $\tilde{\nu}$ = 3259 s br (NH), 3151 w, 1643 m, 1591 s, 1500 m, 1285 vs, 1243 vs, ~1228 sh, 1159 s, 1028 vs, 720 m, 636 s, 574 w, 518 m cm$^{-1}$. – MS ((+)-MALDI-TOF): *m*/*z* (%) = 694.15 (100) [M–$CF_3SO_3$]$^+$, 1539.24 (8) [2 [Cu**L2L2′**(OTf)$_2$]–OTf]. – Anal. for $C_{28}H_{30}CuF_6N_{10}O_6S_2$ (844.27), water-free sample: calcd. C 39.83, H 3.58, N 16.59; S 7.59; found C 39.62, H 3.41, N 16.64, S 7.61.

#### 4.3.3 Diaquabis(2-(1-benzyl-1*H*-1,2,3-triazol-4-yl)-4,5-dihydro-1,3-thiazole)copper(II) bis(trifluoromethanesulfonate) · bis(2-(1-benzyl-1*H*-1,2,3-triazol-4-yl)-4,5-dihydrothiazole) bis(trifluoromethanesulfonato-κ*O*)copper(II), [Cu(L4)$_2$(H$_2$O)$_2$](OTf)$_2$ · [Cu(L4)$_2$(OTf)$_2$]

Ligand **L4** (110 mg, 0.45 mmol) was dissolved in a small volume of ethyl acetate and a saturated solution of copper(II) trifluoromethanesulfonate in ethyl acetate was added. An amorphous light blue precipitate was formed, isolated by filtration and dried at air; yield: 180 mg (94%). The solid was redissolved in the necessary volume of ethyl acetate and this solution was concentrated by slow evaporation with exposure to air. With uptake of water molecules, light blue prismatic crystals suitable for X-ray analysis were formed. The crystals lost water at 180–182°C and melted at 225–228°C. – IR (KBr): $\tilde{\nu}$ = 3447 w br (OH), 3100 w (N–H), 3069 w, 1616 m, 1543 m, 1458 m, 1286 vs, 1246 vs, 1224 s, 1158 s, 1112 m, 1060 m, 1028 s, 721 m, 636 s, 575 w, 518 w cm$^{-1}$. – MS ((+)-MALDI-TOF): *m*/*z* (%) = 700.15 (100) [M–$CF_3SO_3$]. – Anal. for $C_{26}H_{24}CuF_6N_8O_6S_4$ (850.32), water-free sample: calcd. C 36.72, H 2.84, N 13.18; found C 36.55, H 2.87, N 13.27.

#### 4.3.4 Bis(2-(1-benzyl-1*H*-1,2,3-triazol-4-yl)-1,4,5,6-tetrahydropyrimidine)-bis(trifluoromethanesulfonato-κ*O*)copper(II), [Cu(L5)$_2$(OTf)$_2$]

A saturated solution of Cu(OTf)$_2$ in *n*-butanol was added drop by drop to a solution of ligand **L5** (40 mg, 0.16 mmol) in *n*-butanol (3 mL). Diethyl ether was placed on top of the blue butanol layer. After several weeks, deep blue crystal platelets separated which were isolated by filtration with suction, washed with a small volume of diethyl ether and dried at air. Yield: 64 mg (91); M.p. 271–275°C. – IR (KBr): $\tilde{\nu}$ = 3322 br, 3154 w br, 3063 w, 1641 m, 1613 s, 1453 m, 1284 vs, 1256 vs, 1225 vs, 1167 s, 1032 vs, 759 m, 700 s, 639 vs, 576 m, 518 m cm$^{-1}$. – Anal. for $C_{28}H_{30}CuF_6N_{10}O_6S_2$ (844.27): calcd. C 39.83, H 3.58, N 16.59; found C 40.07, H 3.74, N 16.16.

#### 4.3.5 Bis(2-(1-benzyl-1*H*-1,2,3-triazol-4-yl)-4,5-dihydro-1*H*-imidazole)dichloridocopper(II) tetrahydrofuran solvate, [Cu(L1)$_2$Cl$_2$]

Ligand **L1** (34.5 mg, 150 µmol) was dissolved in ethyl acetate (5 mL) and a solution of $CuCl_2$ (10.2 mg, 75 µmol) in ethyl acetate (3 mL) was added. A light green precipitate appeared, which was isolated by filtration with suction, washed with a small volume of pentane and dried at air; yield: 42 mg (95%); M.p. 238–239.5°C (dec.). – IR (KBr): $\tilde{\nu}$ = 3424 m br, 3088 m, 1629 m, 1591 s, 1569 m, 1498 w, 1290 w, 1276 w, 1257 w, 1064 m, 719 m, 578 w cm$^{-1}$. – MS ((+)-MALDI): *m*/*z* (%) = 552.13 (100) [M–Cl]; $C_{24}H_{26}ClCuN_{10}$ requires 552.1326. – $C_{24}H_{26}Cl_2CuN_{10}$ (588.98).

#### 4.3.6 Bis(2-(1-benzyl-1*H*-1,2,3-triazol-4-yl)-4,5-dihydro-1,3-oxazole-κ*N*$^3$)dichloridocopper(II) tetrahydrofuran solvate, [Cu(L3)$_2$Cl$_2$] · THF

Ligand **L3** (16.8 mg, 0.10 mmol) was dissolved in dry THF (3 mL) and a saturated light green solution of $CuCl_2$ in dry THF (2 mL) was gradually added, until the color of the resulting solution had changed from green to deep blue. The solvent was slowly concentrated by evaporation, until dark blue prismatic crystals appeared. They were isolated by filtration with suction and dried at air. Yield: 26.5 mg (80%, for the THF solvate). The crystals lost THF at 106°C and melted at 169–171°C. – $^1$H NMR ($CDCl_3$): $\delta$ = 1.89 (m, 4 H, C$H_2$C$H_2$ of THF), 3.74 (m, 4 H, C$H_2$OC$H_2$ of THF), 4.64 (broad s, 8 H, NC$H_2$C$H_2$O), 5.49 (broad s, 2 H, 5-H), 6.66 (broad s, 4 H, PhC$H_2$), 7.39–7.55 (m, 10 H, $H_{Ph}$) ppm. – Anal. for $C_{24}H_{26}Cl_2CuN_8O_2 \cdot C_4H_8O$ (663.06): calcd. C 50.72, H 4.86, N 16.90; found C 50.64, H 5.02, N 17.35.

#### 4.3.7 Bis(1-benzyl-4-(4,5-dihydro-1*H*-imidazol-2-yl)-1,2,3-triazole)dichloridonickel(II), [Ni(L1)$_2$Cl$_2$]

To a solution of ligand **L1** (38.5 mg, 169 µmol) in 1-butanol (5 mL) was added a solution of $NiCl_2 \times 6H_2O$ (20.1 mg,

**Table 4:** Crystal structure data for [Cu(**L1**)$_2$](OTf)$_2$, [Cu**L2L2′**(OTf)$_2$] and [Cu(**L5**)$_2$(OTf)$_2$].

| | [Cu(L1)$_2$](OTf)$_2$ | [CuL2L2′(OTf)$_2$] · 2H$_2$O | [Cu(L5)$_2$(OTf)$_2$] |
|---|---|---|---|
| Formula | $C_{26}H_{28}CuF_6N_8O_8S_4 \cdot C_{26}H_{24}CuF_6N_8O_6S_4$ | $C_{28}H_{30}CuF_6N_{10}O_6S_2 \cdot 2H_2O$ | $C_{28}H_{30}CuF_6N_{10}O_6S_2$ |
| $M_r$ | 1736.63 | 880.31 | 844.28 |
| Cryst. size, mm$^3$ | 0.27 × 0.22 × 0.12 | 0.30 × 0.16 × 0.13 | 0.25 × 0.11 × 0.09 |
| Temperature, K | 100(2) | 180 | 180(2) |
| Crystal system | monoclinic | monoclinic | monoclinic |
| Space group | $P2_1/c$ | $P2_1$ | $P2_1/c$ |
| $a$, Å | 10.6449(4) | 8.9026(3) | 25.7804(7) |
| $b$, Å | 17.6042(6) | 16.4389(5) | 13.1928(4) |
| $c$, Å | 8.6745(3) | 13.4275(5) | 10.0657(2) |
| $\beta$, ° | 99.510(2) | 104.194(4) | 90.448(2) |
| $V$, Å$^3$ | 1603.22(10) | 1905.10(11) | 3423.41(15) |
| $Z$ | 2 | 2 | 4 |
| $D_{calcd.}$, g cm$^{-3}$ | 1.691 | 1.535 | 1.64 |
| $\mu$, mm$^{-1}$ | 0.906 | 0.772 | 2.86 |
| $F$(000), e | 830 | 902 | 1724 |
| Radiation/$\lambda$, Å | Mo$K_\alpha$/0.71073 | Mo$K_\alpha$/0.71073 | Cu$K_\alpha$/1.54184 |
| $hkl$ range | ±15, ±25, −12:+11 | −8:+11, ±20, −16:+13 | ±31, −14:+16, ±12 |
| $\theta_{max}$, ° | 30.54 | 29.17 | 74.16 |
| Refl. measured | 34440 | 10580 | 20153 |
| Refl. unique/$R_{int}$ | 4903/0.0237 | 6730/0.0229 | 6734/0.0216 |
| Param. Refined | 292 | 498 | 486 |
| $R(F)/wR(F^2)$[a] (all refl.) | 0.0385/0.0976 | 0.0524/0.1296 | 0.0629/0.1423 |
| GoF ($F^2$)[a] | 1.080 | 1.015 | 1.062 |
| $x$(Flack) | – | −0.005(14) | – |
| $\Delta\rho_{fin}$ (max/min), e Å$^{-3}$ | 0.65/−0.79 | 0.69/−0.41 | 1.32/−0.51 |
| CCDC no. | 1446997 | 1446994 | 1447013 |

[a] $R(F) = \Sigma||F_o|-|F_c||/\Sigma|F_o|$; $wR(F^2) = [\Sigma w(F_o^2-F_c^2)^2/\Sigma w(F_o^2)^2]^{1/2}$; GoF = $S = [\Sigma w(F_o^2-F_c^2)^2/(n_{obs}-n_{param})]^{1/2}$.

84 µmol) in 1-butanol (3 mL). On standing for about 3 weeks, light green crystals appeared which were collected by filtration with suction and dried at air (37 mg, 75% yield). The crystals did not melt up to 326°C, only a color change to dark brown was observed beyond this temperature. – IR (KBr): $\tilde{\nu}$ = 3164 s (N–H), 3091 m, 1641 s, 1580 s, 1497 m, 1479 m, 1456 m, 1282 m, 1263 m, 1243 m, 1067 m, 1032 m, 720 m cm$^{-1}$. – MS ((+)-MALDI): $m/z$ (%) = 547.14 (99) [M–Cl], 511.16 (100) [M–2Cl–H]; required: 547.14, 511.16. – Anal. for $C_{24}H_{26}Cl_2N_{10}Ni$ (584.13): calcd. C 49.35, H 4.49, N 23.98. A correct analysis could not be obtained.

## 4.4 X-ray structure determinations

Suitable single crystals of the investigated complexes were obtained as described above in the synthetic procedures. Data collection was performed on an Oxford SuperNova diffractometer (dual source, Atlas CCD) at the University of Ulm and a Bruker Kappa APEX II Duo diffractometer at the University of Stuttgart. Software for structure solution and refinement: SHELXS/L-97 [38] and SHELXL-2014/6 [39]; molecule plots: ORTEP-III [40, 41] and MERCURY [42]. In all ORTEP plots, the size of the displacement ellipsoids represents 30% probability. In the refinement procedure, hydrogen atoms were usually placed in geometrically calculated positions and treated as riding on their bond neighbors in the refinement. NH and OH hydrogen atom positions were taken from a difference-Fourier electron density map and were refined. Further details are provided in Tables 4 and 5. For [Cu**L2L2′**(OTf)$_2$] · 2H$_2$O, which crystallizes in the noncentrosymmetric space group $P2_1$, the correct absolute structure is supported by the value of the Flack parameter.

CCDC 1446994, 1446997 and 1447013–1447016 contain the supplementary crystallographic data for this paper. These data can be obtained free of charge from The Cambridge Crystallographic Data Centre *via* www.ccdc.cam.ac.uk/data_request/cif.

**Table 5:** Crystal structure data for $[Cu(\mathbf{L4})_2(H_2O)_2](OTf)_2 \cdot [Cu(\mathbf{L4})_2(OTf)_2]$, $[Cu(\mathbf{L3})_2Cl_2] \cdot THF$ and $[Ni(\mathbf{L1})_2Cl_2]_2$.

| | $[Cu(L4)_2(H_2O)_2](OTf)_2 \cdot [Cu(L4)_2(OTf)_2]$ | $[Cu(L3)_2Cl_2] \cdot THF$ | $[Ni(L1)_2Cl_2]$ |
|---|---|---|---|
| Formula | $C_{26}H_{26}CuF_6N_8O_7S_4$ | $C_{24}H_{24}Cl_2CuN_8O_2 \cdot C_4H_8O$ | $C_{24}H_{26}Cl_2N_{10}Ni$ |
| $M_r$ | 868.33 | 663.07 | 584.16 |
| Cryst. size, mm³ | 0.22 × 0.17 × 0.08 | 0.22 × 0.17 × 0.15 | 0.16 × 0.09 × 0.06 |
| Temperature (K) | 150(2) | 150(2) | 150(2) |
| Crystal system | triclinic | monoclinic | orthorhombic |
| Space group | $P\bar{1}$ | $C2/c$ | $Pbcn$ |
| $a$, Å | 7.7753(3) | 23.5405(6) | 11.9140(2) |
| $b$, Å | 13.8579(5) | 8.8545(2) | 9.5622(2) |
| $c$, Å | 16.3674(7) | 15.5836(4) | 22.9451(4) |
| $\alpha$, ° | 85.302(3) | 90 | 90 |
| $\beta$, ° | 89.710(3) | 113.347(3) | 90 |
| $\gamma$, ° | 86.194(3) | 90 | 90 |
| $V$, Å³ | 1753.77(12) | 2982.28(13) | 2613.99(7) |
| $Z$ | 2 | 4 | 4 |
| $D_{calcd.}$, g cm⁻³ | 1.644 | 1.477 | 1.484 |
| $\mu$, mm⁻¹ | 0.948 | 0.957 | 0.324 |
| $F$(000), e | 882 | 1372 | 1208 |
| Radiation/$\lambda$, Å | Mo$K_\alpha$/0.71073 | Mo$K_\alpha$/0.71073 | Cu$K_\alpha$/1.54184 |
| $hkl$ range | −9:+8, ±16, ±19 | −28:+30, −12:+9, −18:+19 | ±14, −11:+10,−28:+20 |
| $\theta_{max}$, ° | 24.71 | 29.18 | 73.89 |
| Refl. measured | 19843 | 8706 | 7812 |
| Refl. unique/$R_{int}$ | 5972/0.0387 | 3523/0.0204 | 2586/0.0224 |
| Param. refined | 480 | 205 | 172 |
| $R(F)/wR(F^2)$[a] (all refl.) | 0.0623/0.0958 | 0.0451/0.1038 | 0.0340/0.0724 |
| GoF ($F^2$)[a] | 0.952 | 1.047 | 1.035 |
| $\Delta\rho_{fin}$ (max/min), e Å⁻³ | 0.90/−0.67 | 0.83/−0.61 | 0.26 /−0.18 |
| CCDC no. | 1447014 | 1447015 | 1447016 |

[a] $R(F) = \Sigma||F_o|-|F_c||/\Sigma|F_o|$; $wR(F^2) = [\Sigma w(F_o^2-F_c^2)^2/\Sigma w(F_o^2)^2]^{1/2}$; GoF = $S = [\Sigma w(F_o^2-F_c^2)^2/(n_{obs}-n_{param})]^{1/2}$.

**Acknowledgments:** We thank Bernhard Müller and Dieter Sorsche for the X-ray data collection at Ulm.

# References


[1] G. Aromi, L. A. Barrios, O. Roubeau. P. Gamez, *Coord. Chem. Rev.* **2011**, *255*, 485.
[2] J. D. Crowley, D. A. McMorran, *Top. Heterocycl. Chem.* **2012**, *28*, 31.
[3] J. G. Haasnoot, *Coord. Chem. Rev.* **2000**, *200–202*, 131.
[4] M. H. Klingele, S. Brooker, *Coord. Chem. Rev.* **2003**, *241*, 119.
[5] E. A. Popova, R. E. Trifonov, V. A. Ostrovskii, *Arkivoc* **2012**, (*i*), 45.
[6] M. Meldal, C. W. Tornoe, *Chem. Rev.* **2008**, *108*, 2952.
[7] D. Schweinfurth, N. Deibel, F. Weisser, B. Sarkar, *Nachrichten aus der Chemie* **2011**, *59*, 937.
[8] H. Struthers, T. L. Mindt, R. Schibli, *Dalton Trans.* **2010**, *39*, 675.
[9] M. Mydlak, C. Bizzarri, D. Hartmann, W. Sarfert, G. Schmid, L. De Cola, *Adv. Funct. Mater.* **2010**, *20*, 1812.
[10] J. D. Crowley, P. H. Bandeen, *Dalton Trans.* **2010**, *39*, 612.
[11] S. Q. Bai, S. Leelasubcharoen, X. Chen, L. L. Koh, J.-L. Zuo, T. S. A. Hor, *Crystal. Growth Des.* **2010**, *10*, 1715.
[12] Z. Benkhellat, M. Allali, M. Beley, E. Wenger, M. Bernard, N. Parizel, K. Selmeczi, J.-P. Joly, *New J. Chem.* **2014**, *38*, 419.
[13] P. I. P. Elliott, *Organomet. Chem.* **2014**, *39*, 1.
[14] D. Wang, D. Denux, J. Ruiz, D. Astruc, *Adv. Synth. Catal.* **2013**, *355*, 129.
[15] B. R. Buckley, H. Heaney, *Top. Heterocycl. Chem*. **2012**, *28*, 1.
[16] D. Mendoza-Espinosa, G. E. Negrón-Silva, D. Angeles-Beltrán, A. Álvarez-Hernández, O. R. Suárez-Castillo, R. Santillán, *Dalton Trans.* **2014**, *43*, 7069.
[17] L. Li, C. S. B. Gomes, P. S. Lopes, P. T. Gomes, H. P. Diogo, J. R. Ascenso, *Eur. Polymer J.* **2011**, *47*, 1636.
[18] A. Pfaltz, *Acc. Chem. Res.* **1993**, *26*, 339.
[19] R. E. Lowenthal, A. Abiko, S. Masamune, *Tetrahedron Lett.* **1990**, *31*, 6005.
[20] R. E. Lowenthal, S. Masamune, *Tetrahedron Lett.* **1991**, *32*, 7373.
[21] D. A. Evans, K. A. Woerpel, M. M. Hinman, M. M. Faul, *J. Am. Chem. Soc.* **1991**, *113*, 726.
[22] J. S. Johnson, D. A. Evans, *Acc. Chem. Res.* **2000**, *33*, 325.
[23] R. Hayashi, X. Jin, G. R. Cook, *Bioorg. Med. Chem. Lett.* **2007**, *17*, 6864.
[24] W. Weingärtner, G. Maas, *Eur. J. Org. Chem.* **2012**, 6372.
[25] G. Valdomir, J. I. Padrón, J. M. Padrón, V. S. Martín, D. Davyt, *Synthesis* **2014**, *46*, 2451.
[26] G. A. Lawrance, *Chem. Rev.* **1986**, *86*, 17.
[27] D. H. Johnston, D. F. Shriver, *Inorg. Chem.* **1993**, *32*, 1045.
[28] P. L. Dedert, J. S. Thompson, J. A. Ibers, T. J. Marks, *Inorg. Chem.* **1982**, *21*, 969.
[29] J. S. Haynes, S. J. Rettig, J. R. Sams, J. Trotter, R. C. Thompson, *Inorg. Chem.* **1988**, *27*, 1237.

[30] T. Otieno, S. J. Rettig, R. C. Thompson, J. Trotter, *Can. J. Chem.* **1989**, *67*, 1964.
[31] T. Otieno, S. J. Rettig, R. C. Thompson, J. Trotter, *Can. J. Chem.* **1990**, *68*, 1901.
[32] G. A. van Albada, W. J. J. Smeets, A. L. Spek, J. Reedijk, *Inorg. Chim. Acta* **1997**, *260*, 151.
[33] B. J. Hathaway, D. E. Billing, *Coord. Chem. Rev.* **1970**, *3*, 143.
[34] Y. Shvedenkov, M. Bushuev, G. Romanenko, L. Lavrenova, V. Ikorskii, P. Gaponik, S. Larionov, S. *Eur. J. Inorg. Chem.* **2005**, *9*, 1678.
[35] D. A. Evans, S. J. Miller, T. Lectka, P. v. Matt, *J. Am. Chem. Soc.* **1999**, *121*, 7559.
[36] N. Siddiqui, W. Ahsan, M. S. Alam, R. Ali, S. Jain, B. Azad, J. Akhtar, *Int. J. Pharm. Sc. Rev. Res.* **2011**, *8*, 161.
[37] A. D. Moorhouse, J. E. Moses, *ChemMedChem* **2008**, *3*, 715.
[38] G. M. Sheldrick, *Acta Crystallogr.* **2008**, *A64*, 112.
[39] G. M. Sheldrick, *Acta Crystallogr.* **2015**, *C71*, 3.
[40] C. K. Johnson, M. N. Burnett, ORTEP-III (version 1.0.2), Oak Ridge Thermal Ellipsoid Plot Program for Crystal Structure Illustrations, Rep. ORNL-6895, Oak Ridge National Laboratory, Oak Ridge, TN (USA) **1996**.
[41] L. J. Farrugia, *J. Appl. Crystallogr.* **2012**, *45*, 849.
[42] MERCURY (version 3.5), Cambridge Crystallographic Data Centre, Cambridge (U.K.), **2014**.

# Graphical synopsis

Sven Schröder, Wolfgang Frey and Gerhard Maas

**2-(1,2,3-Triazol-4-yl)-imidazoline, -oxazoline, -thiazoline and -tetrahydropyrimidine as ligands in copper(II) and nickel(II) complexes**

DOI 10.1515/znb-2016-0026
Z. Naturforsch. 2016; x(x)b: xxx–xxx

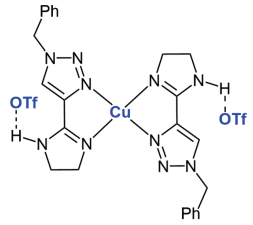


[Cu(**L1**)$_2$](OTf)$_2$

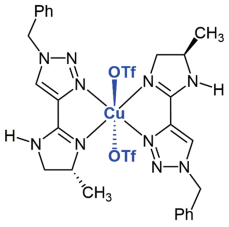


[Cu**L2L2′**(OTf)$_2$]

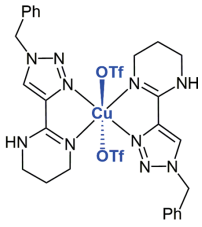


[Cu(**L5**)$_2$(OTf)$_2$]